First-Principles Calculations of the Urbach Tail in the Optical Absorption Spectra of Silica Glass

B. Sadigh, P. Erhart, D. Åberg, A. Trave, E. Schwegler, and J. Bude

Phys. Rev. Lett. **106**, 027401 — Published 10 January 2011

DOI: 10.1103/PhysRevLett.106.027401

First principles calculations of the Urbach tail in the optical absorption of silica glass

B. Sadigh, P. Erhart, D. Åberg, A. Trave, E. Schwegler, and J. Bude
Lawrence Livermore National Laboratory, Chemistry, Materials and Life Sciences Directorate, Livermore, CA, 94550

We present density-functional theory calculations of the optical absorption spectra of silica glass for temperatures up to 2400 K. The calculated spectra exhibit exponential tails near the fundamental absorption edge that follow the Urbach rule, in good agreement with experiments. We discuss the accuracy of our results by comparing to hybrid exchange correlation functionals. By deriving a simple relationship between the exponential tails of the absorption coefficient and the electronic density-of-states, we establish a direct link between photoemission and absorption spectra near the absorption edge. This relationship is subsequently employed to determine the lower bound to the Urbach regime. In this frequency interval the optical absorption is Poisson distributed with very large statistical fluctuations. Finally, we identify the upper bound to the Urbach regime as the frequency at which the transition to a Poisson distribution occurs.

PACS numbers: 78.40.Pg, 78.20.Bh, 71.23.An, 71.15.Mb

At finite temperatures absorption spectra of insulators exhibit an exponential energy dependence near the fundamental absorption edge that varies with temperature according to [1]

$$\overline{\alpha}(\omega, T) = \alpha_0 \exp\left[-\sigma \frac{\hbar\omega_0(T) - \hbar\omega}{kT}\right]. \qquad (1)$$

Here $\omega_0(T)$ is a linear function of temperature, which at zero K is defined to be the optical gap, while σ and α_0 are constants that can be extracted from experiments. The Urbach rule, Eq. (1), has been observed universally in crystals as well as glasses. Extensive research over many decades [2] has shown that it arises from transitions between localized electronic levels resulting from fluctuations of band-edge states into the band gap and extended states [3, 4]. In a pioneering work on amorphous Si, the fluctuations in the single-particle energies at the band edges obtained from *ab-initio* molecular-dynamics (MD) simulations in the local density approximation (LDA) were found to be in good agreement with experimentally measured band tail widths.[5] While this demonstrates the applicability of *ab-initio* MD in the adiabatic approximation, the question remains whether single-particle theories can provide a quantitative description of the Urbach tail in wide band gap materials. On the one hand, it has been shown that charge localization due to excitonic binding is responsible for the low-energy absorption peaks in these systems [6, 7]. On the other hand, at elevated temperatures the phonon-induced localization of the single-particle states may very well be sufficient to provide a quantitative description of the observed exponential tails in optical spectra. In this Letter we address this issue by investigating the Urbach rule in defect-free silica glass using *ab-initio* MD simulations. A detailed comparison with experiments shows that the Urbach behavior can be accurately described within a single-particle picture for this system.

The present work has been motivated by the need to develop a better understanding of the process of laser damage to silica optics, which is of importance to diverse fields ranging from opto-electronics to inertial confinement fusion. Recently, the role of temperature has been emphasized by experiments where damage was generated far below the bulk material threshold by photons of energy 3.55 eV at about 2200 K [11]. The Urbach rule plays a crucial role here since the exponential dependence of absorption on temperature in Eq. (1) necessitates the existence of a critical temperature T_c, at which the glass absorbs more photon energy than it can dissipate leading to thermal run-away and macroscopic damage [11]. However, extrapolation of experimental spectra [12] predicts a T_c that is several hundred K higher than the measured value. Therefore better understanding of the kinetics of absorption in the Urbach regime is needed. The objective of this Letter is to study the physical processes that lead to absorption in a temperature and energy range for which experiments are not available. The key finding is that in the Urbach regime absorption is best described as a Poisson process of localized bursts that occur at sub-terahertz frequencies. On this basis, quantitative models for prediction of T_c can be obtained.

The MD simulations presented in this work are performed within DFT-GGA using the PW91 parametrization [13, 14] as implemented in the Vienna ab-initio simulation package [15] using the projector augmented wave method [16]. Calculations involve supercells containing 24 SiO_2 formula units and the Brillouin zone is sampled by a $2\times2\times2$ Monkhorst-Pack k-point grid. In order to obtain a realistic glass model, we started from a liquid silica model obtained previously [17], which was quenched down to zero K over a period of about 10 ps. The examination of the electronic structure of the resulting configurations revealed defect states due to the presence of stretched and broken bonds. [8] The defect states were eliminated from the model by optimization via a bond-switching Monte Carlo (BSMC) technique [9, 18]. Several BSMC-refined configurations were generated, each representing a random network with fixed bond lengths and angles. Subsequently, the configurations were structurally relaxed to the local GGA total energy minimum. The final glass model that was chosen from this set had preserved its bond lengths and angles after the relaxation process. The electronic density-of-states (DOS) of this configuration is shown in Fig. 1(a) in comparison with the PBE0 hybrid functional, which incorporates 25% exact exchange [19, 20]. The GGA DOS includes a band gap shift of $\Delta_g = 2.6$ eV to account for the systematic underestimation of the band gap. We find excellent agree-

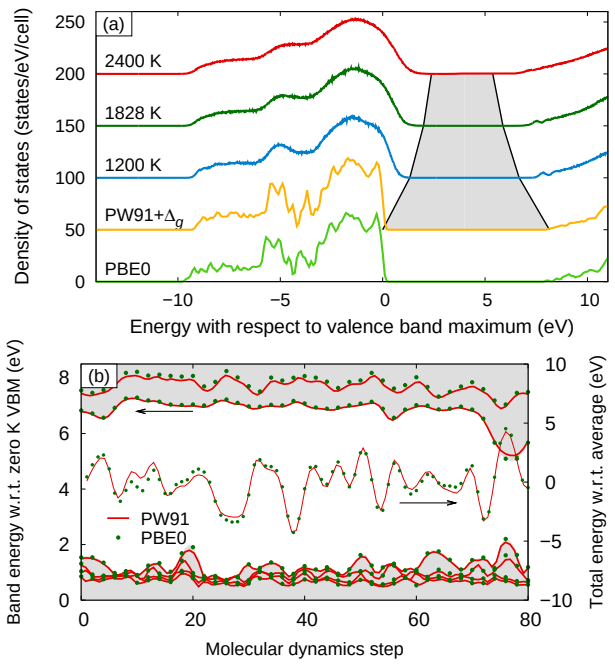

FIG. 1: (a) Density-of-states for the perfect glass at zero K calculated using the PBE0 hybrid functional and the PW91 functional with scissors correction (PW91+Δ_g. Also shown is the density of states obtained from MD simulations at three different temperatures using PW91+Δ_g. (b) Single-particle energies of the four topmost valence band states and the two lowermost conduction band states (thick lines, large circles) as well as the total energy (thin lines, small circles) along a MD trajectory (generated using PW91) obtained using a hybrid functionals (PBE0) in comparison with the PW91+Δ_g approach.

ment between the two calculations for the perfect glass. As a further test, we have explicitly compared the time evolution of the band edge states and the total energy at 2200 K, calculated from GGA with PBE0 as well as HSE06 [21] (a hybrid functional that includes screened exchange) calculations [Fig. 1(b)]. It appears that with a constant band gap shift (2.6 eV for GGA and 0.9 eV for HSE06), all calculations can be brought in agreement with each other. A similar conclusion was reached in studying point defects [10].

The absorption coefficient for photons of energy $\hbar\omega$ of an atomic configuration $\boldsymbol{X}$, can be calculated as follows

$$\alpha(\omega;\boldsymbol{X}) = \sqrt{2}\frac{\omega}{c}\sqrt{|\epsilon(\omega;\boldsymbol{X})| - \epsilon_R(\omega;\boldsymbol{X})}, \qquad (2)$$

where $\epsilon(\omega;\boldsymbol{X})$ is the complex dielectric function $\epsilon = \epsilon_R + i\epsilon_I$. In the velocity gauge, ϵ_I can be directly computed from the single-particle wave functions and energies [22, 23] as well as their occupancies $f_{n\boldsymbol{k}}$ as follows

$$\epsilon_I(\omega;\boldsymbol{X}) = \frac{4\pi^2 e^2}{m_e^2\omega^2}\sum_{n,n'}(f_{n'\boldsymbol{k}} - f_{n\boldsymbol{k}})\left|M^{\boldsymbol{k}}_{nn'}(\boldsymbol{X})\right|^2 \times \delta\left(\Delta_g + e_{n'\boldsymbol{k}}(\boldsymbol{X}) - e_{n\boldsymbol{k}}(\boldsymbol{X}) - \hbar\omega\right), \qquad (3)$$

where $M^{\boldsymbol{k}}_{nn'}(\boldsymbol{X})$ are the polarization-averaged dipole matrix elements between the states $n\boldsymbol{k}$ in the valence band and $n'\boldsymbol{k}$ in the conduction band. The summations in Eq. (3) run over bands and spins, and the real part ϵ_R can be obtained from ϵ_I through a Kramers-Kronig relation. Since the latter involves an integration over the entire frequency spectrum, we have included as many as 1000 unoccupied bands in our calculations.

At finite temperatures, the response functions as well as the DOS are calculated by classical ensemble averaging over ionic displacements in the Born-Oppenheimer approximation, treating the electronic transitions as instantaneous. Figure 1(a) shows the average DOS at three different temperatures. The gray region depicts the narrowing of the band gap with increasing temperature, leading to an exponential increase of the free carrier densities. While at 2400 K the density of free carriers can be as large as $10^{17}\,\mathrm{cm}^{-3}$, it is still too small to have any measurable impact on the absorption in the Urbach regime.

The DOS can be linked to optical absorption via the joint density-of-states (JDOS), which at zero K is defined as $J(\omega) = \int \rho_v(\omega')\rho_c(\omega'+\omega)\,d\omega'$, where $\rho_{v(c)}(\omega)$ is the DOS of the valence (conduction) bands. At finite temperatures, a direct relationship between the JDOS and the DOS only exists if the fluctuations in the valence and the conduction bands are independent

$$\langle\mathcal{J}(\omega)\rangle_T \approx \int \langle\rho_v(\omega')\rangle_T \langle\rho_c(\omega'+\omega)\rangle_T \; d\omega'. \qquad (4)$$

We find that the above is a very good approximation over the entire frequency range, which implies that knowledge of the DOS is sufficient to determine of the JDOS. In the Urbach regime, the JDOS can be linked to the dielectric function via

$$\langle\epsilon_I(\omega)\rangle_T \approx \overline{\mu}(T)\,\langle\mathcal{J}(\omega)\rangle_T\,. \qquad (5)$$

This is illustrated in Fig. 2(a), where the low-frequency exponential tail of the dielectric function and the JDOS are shown to coincide when the latter is scaled by a temperature-dependent effective dipole transition probability (DTP) $\overline{\mu}(T)$. This result suggests that the frequency dependence of the Urbach tail originates from the exponential decay of the JDOS, while the matrix elements provide an effective temperature-dependent prefactor. As shown in the inset of Fig. 2(a), $1/\overline{\mu}(T)$ decreases linearly with temperature, resulting in a reduction by a factor of two between 1200 and 2400 K. As was noted by Chang *et al.* [7], the inclusion of excitonic effects has a small impact on the JDOS. The excitonic peaks that appear in the optical absorption of α-quartz are instead due to enhanced oscillator strength of transitions to correlated electron-hole states that are spatially localized. The inclusion of electron-hole interactions in the calculations may thus modify the prefactor $\overline{\mu}(T)$ but not the overall shape of the Urbach tail. Furthermore, we expect the inclusion of electron-hole interactions to lead only to small modifications of $\overline{\mu}(T)$ as the single-particle states in the tail region are already localized due to phonons.

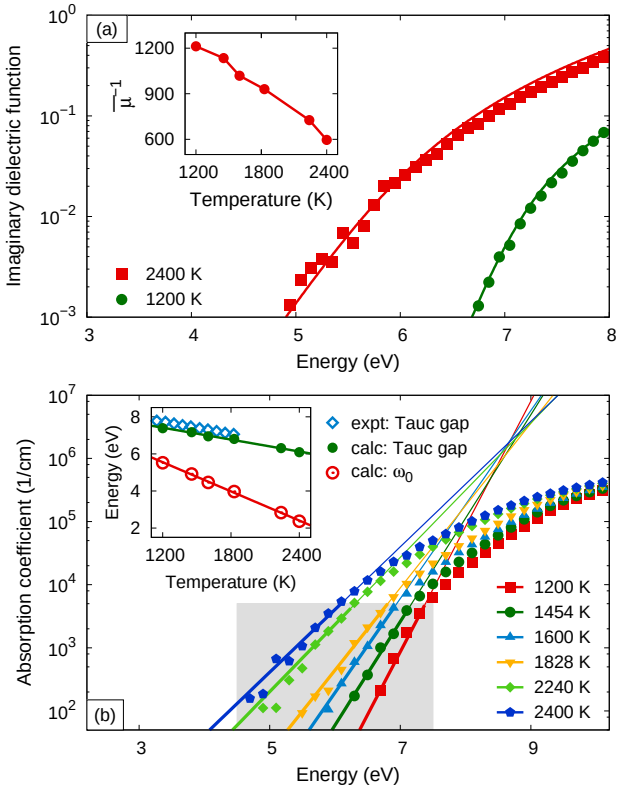

FIG. 2: (a) JDOS rescaled by $\overline{\mu}(T)$ (solid lines) and imaginary dielectric function (symbols). The inset shows $\overline{\mu}(T)^{-1}$ as a function of temperature. (b) Absorption coefficient in the Urbach regime calculated using PW91+Δ_g. The inset shows the result of a fit to Eq. (1) and the comparison with the experimental data from Saito and Ikushima [12]. The shaded region depicts the Urbach regime.

After obtaining the dielectric functions at different temperatures, it is straightforward to calculate the absorption spectra shown in Fig. 2(b) via Eq. (2). Fitting the exponential tails of these spectra to Eq. (1) yields a linear temperature dependence for $\omega_0(T)$ as shown in the inset of Fig. 2(b), extending the Urbach rule to 2400 K. The fit also gives $\sigma = 0.473$ in fair agreement with the experimental value of $\sigma = 0.585$. [12] The Tauc gap, which is the threshold energy for the onset of extended-to-extended electronic transitions, can be extracted as well. Following Ref. 12, where the Tauc gap was defined as the photon energy corresponding to $5 \times 10^3\,\mathrm{cm}^{-1}$ absorption, one obtains the data shown in the inset of Fig. 2(b) again demonstrating excellent agreement.

The good agreement between the calculated and experimental Tauc gaps is the most definite evidence that a single-particle picture is sufficient for describing optical absorption in the Urbach regime. Since excitonic effects lead to increased absorption at low energies, our calculated Tauc gaps would have been significantly higher than experiment if electron-hole interactions were essential. Following the same argument, it is expected that excitonic effects should extend the Urbach tail to lower frequencies by lowering σ in Eq. (1). Yet, since our calculations already underestimate σ, this deviation is unlikely to be due to excitonic effects.

In the Urbach regime the ratio $\langle\epsilon_I(\omega)\rangle_T / \langle\epsilon_R(\omega)\rangle_T \ll 1$. A first order Taylor expansion of Eq. (2) with respect to this quantity yields the following expressions for the absorption coefficient

$$\langle\alpha(\omega)\rangle_T \approx \frac{\omega}{c}\frac{\langle\epsilon_I(\omega)\rangle_T}{\sqrt{\langle\epsilon_R(\omega)\rangle_T}} \approx \frac{\omega}{c}\frac{\overline{\mu}(T)}{\sqrt{\langle\epsilon_R(0)\rangle_T}}\langle\mathcal{J}(\omega)\rangle_T\,. \quad (6)$$

The second approximation above is obtained by a zeroth order expansion about the static dielectric constant $\langle\epsilon_R(0)\rangle_T$, and utilizes our earlier finding that the Urbach tail of the imaginary dielectric function can be obtained from the JDOS, see Eq. (5). Using Eqs. (4) and (6), we can establish a simple relationship between the absorption coefficient and the DOS in the vicinity of the absorption edge, where the temperature dependence of the prefactor mainly enters through the effective DTP $\overline{\mu}(T)$, while $\langle\epsilon_R(0)\rangle_T$ varies only weakly with temperature, i.e. from 1.81 at 0 K to 1.99 at 2400 K. Since experimentally the DOS is obtained via photoemission spectroscopy, the above result provides a direct link between photoemission and optical absorption experiments in the Urbach regime.

We now discuss fluctuations in the optical absorption due to atomic vibrations. A lower bound can be obtained by using Eq. (6) and only considering fluctuations in the JDOS. Figure 3(a) shows unexpectedly large fluctuations in the JDOS in the Urbach regime with the ratio $\langle\mathcal{J}^2(\omega)\rangle_T / \langle\mathcal{J}(\omega)\rangle_T^2$ reaching 10^4. Hence the standard deviation from mean absorption in the Urbach tail can be up to two orders of magnitude larger than $\langle\alpha(\omega)\rangle_T$.

The large fluctuations in the Urbach regime originate from the discrete nature of the JDOS itself. Even if $\langle\mathcal{J}(\omega)\rangle_T \ll 1$, there can only exist an integer number $\mathcal{N}$ of pairs of electronic states available for transition at any instant of time. Hence the absorption coefficient locally vary between zero and $\overline{\mu}^2 \times \mathcal{N}$, which can amount to fluctuations much larger than the mean value $\langle\mathcal{J}\rangle_T$ itself. This behavior is a consequence of the quantum nature of matter. Let us define an absorption event as the instant of time when $\mathcal{N} > 0$. Whenever absorption events occur rarely enough to be considered independent, the absorption process is Poisson distributed with $\langle\mathcal{J}(\omega)\rangle_T$ interpreted as the average rate of occurrence. An important signature of the Poisson distribution is that its standard deviation is equal to the square root of its average. As shown in Fig. 3(b) in the Urbach regime, this is indeed the case with the ratio sharply decreasing for higher energies. The abrupt transition provides a natural definition for the upper bound to the Urbach region ω_U. Figure 3(d) shows that in the temperature range considered here, ω_U decreases linearly. These observations bestow the finite-temperature JDOS in the Urbach tail with distinct physical significance as it represents the average rate of occurrence of absorption events in this frequency interval.

The Urbach tail region is a closed frequency interval in the optical spectrum. Above, we have determined the upper bound for this interval. We can also determine its lower bound using Eq. (4) to compute $\langle\mathcal{J}(\omega)\rangle_T$ down to very small values with good statistical accuracy. Figure 3(c) shows that at

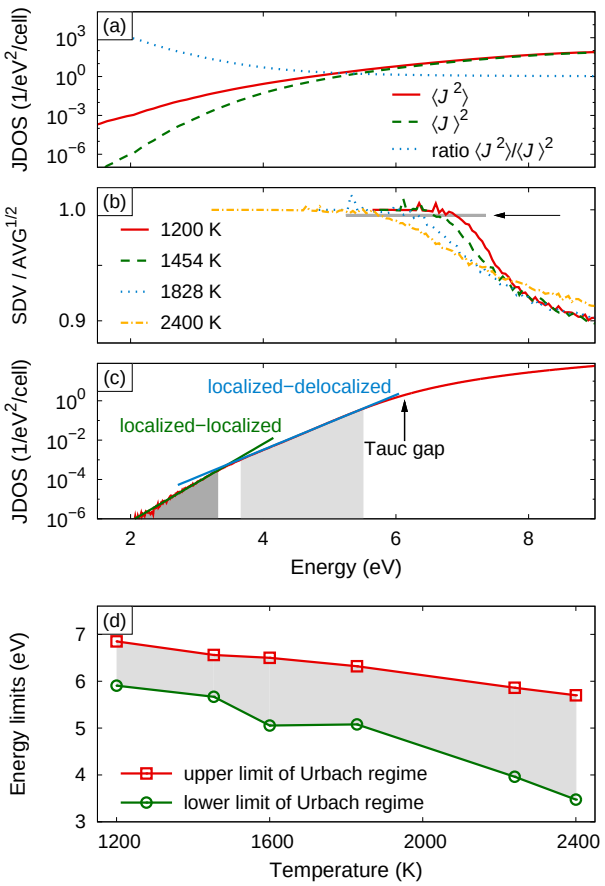

FIG. 3: (a) First and second moment of the joint density of states (JDOS) as well as their ratio at 2400 K. (b) In the Urbach regime the standard deviation of the JDOS equals the square root of the average indicative of a Poisson distribution. The energy at which the ratio deviates from one (indicated by the arrow) provides a simple measure for the upper limit of the Urbach regime. (c) At low energies the JDOS exhibits two distinct regions corresponding to localized-delocalized (Urbach regime) and localized-localized transitions. Each region is described by a different exponential whose crossing point defines a lower limit for the Urbach regime. Note that the Tauc gap lies above the region in which the JDOS exhibits exponential tails. (d) Upper and lower limits of the Urbach regime extracted from the data presented in (b) and (c).

very low energies the slope of the signature exponential decay of the Urbach tail changes. The frequency ω_L at which this transition occurs can be used to identify the lower bound of the Urbach regime, the temperature dependence of which is shown in Fig. 3(d). This lower-frequency region corresponds to transitions between localized levels in the exponential tails of the valence and the conduction bands while the Urbach tail originates from transitions between localized tail states and extended band-like states.

Finally, let us discuss modeling laser heating in silica which can be described by a heat conduction equation with a source term. The latter incorporates energy deposition by linear coupling to laser light, $\overline{\alpha}\,(\omega,T)\,I(\mathbf{r})$, where $I(\mathbf{r})$ is the laser light intensity. Neglecting fluctuations, this term can be parametrized by $\overline{\alpha}(\omega,T) = \langle\alpha(\omega)\rangle_T$. However, the rare event nature of absorption in the Urbach regime calls for $\overline{\alpha}(\omega,T)$ to be treated as a discrete Poisson process, where at a rate proportional to $\langle\mathcal{J}(\omega)\rangle_T$ an absorption event of strength $\omega\overline{\mu}^2/c\sqrt{\langle\epsilon_R(0)\rangle_T}$ takes place. The large fluctuations introduced in this way can reduce the predicted thermal run-away temperature leading to better agreement with experiments.

This work performed under the auspices of the U.S. Department of Energy by Lawrence Livermore National Laboratory under Contract DE-AC52-07NA27344 with support from the Laboratory Directed Research and Development Program.

[1] F. Urbach, Phys. Rev. **92**, 1324 (1953).
[2] T. H. Keil, Phys. Rev. **144**, 582 (1966); C. M. Soukoulis, M. H. Cohen, and E. N. Economou, Phys. Rev. Lett. **53**, 616 (1984); B. I. Halperin and M. Lax, Phys. Rev. **148**, 722 (1966).
[3] T. A. Abtew and D. A. Drabold, Phys. Rev. B **75**, 045201 (2007).
[4] Y. Pan, F. Inam, M. Zhang, and D. A. Drabold, Phys. Rev. Lett. **100**, 206403 (2008).
[5] D. A. Drabold, P. A. Fedders, S. Klemm, and O. F. Sankey, Phys. Rev. Lett. **67**, 2179 (1991).
[6] L. X. Benedict, and E. .L. Shirley, Phys. Rev. B **59**, 5441 (1999).
[7] E. K. Chang, M. Rohlfing, and S. G. Louie, Phys. Rev. Lett. **85**, 2613 (2000).
[8] G. Pacchioni and G. Ieranó, Phys. Rev. B **56**, 7304 (1997).
[9] T. Bakos, S. N. Rashkeev, and S. T. Pantelides, Phys. Rev. B **70**, 075203 (2004).
[10] A. Alkauskas, P. Broqvist, and A. Pasquarello, Phys. Rev. Lett. **101**, 046405 (2008).
[11] J. Bude, G. Guss, M. Matthews, and M. L. Spaeth, SPIE proceedings **6720**, 672009 (2007).
[12] K. Saito and A. J. Ikushima, Phys. Rev. B **62**, 8584 (2000).
[13] J. P. Perdew and Y. Wang, Phys. Rev. B **33**, 8800 (1986).
[14] J. P. Perdew, in *Electronic structure of solids*, edited by P. Ziesche and H. Eschrig (Akademie Verlag, Berlin, 1991), p. 11.
[15] G. Kresse and J. Hafner, Phys. Rev. B **47**, 558 (1993); *ibid.* **49**, 14251 (1994); G. Kresse and J. Furthmüller, *ibid.* **54**, 11169 (1996); Comp. Mater. Sci. **6**, 15 (1996).
[16] P. E. Blöchl, Phys. Rev. B **50**, 17953 (1994); G. Kresse and D. Joubert, *ibid.* **59**, 1758 (1999).
[17] A. Trave, P. Tangney, S. Scandolo, A. Pasquarello, , and R. Car, Phys. Rev. Lett. **89**, 245504 (2002).
[18] F. Wooten, K. Winer, and D. Weaire, Phys. Rev. Lett. **54**, 1392 (1985).
[19] J. P. Perdew, K. Burke, and M. Ernzerhof, Phys. Rev. Lett. **77**, 3865 (1996), erratum, *ibid.* **78**, 1396(E) (1997).
[20] M. Ernzerhof, J. P. Perdew, and K. Burke, Int. J. Quantum Chem. **64**, 285 (1997); M. Ernzerhof and G. E. Scuseria, J. Chem. Phys. **110**, 5029 (1999); C. Adamo and V. Barone, *ibid.* **116**, 6158 (1999).
[21] J. Heyd, G. E. Scuseria, and M. Ernzerhof, J. Chem. Phys. **118**, 8207 (2003), erratum: *ibid.* **124**, 219906 (2006).
[22] R. Del Sole and R. Girlanda, Phys. Rev. B **48**, 11789 (1993).
[23] Z. H. Levine and D. C. Allan, Phys. Rev. B **43**, 4187 (1991).